

# **NOAA Atlas NESDIS 40**



## **YEARLY AND YEAR-SEASON UPPER OCEAN TEMPERATURE ANOMALY FIELDS, 1948-1998**

Sydney Levitus, Cathy Stephens, John Antonov, and Timothy P. Boyer  
National Oceanographic Data Center  
Ocean Climate Laboratory

Silver Spring, MD  
October 2000

**U.S. DEPARTMENT OF COMMERCE**  
**Norman Y. Mineta, Secretary**

**National Oceanic and Atmospheric Administration**  
**D. James Baker, Under Secretary**

National Environmental Satellite, Data, and Information Service  
Gregg Withee, Assistant Administrator



## Contents

Acknowledgments .....	vi
Abstract .....	1
1. Introduction .....	1
2. Data processing and objective analysis .....	2
3. Interannual standard deviation .....	3
4. Summary .....	4
5. References .....	4

## List of Figures

- [illegible]

- Figure 17. Interannual standard deviation ( $^{\circ}\text{C}$ ) of temperature at 800 m depth based on year-season anomaly fields for 1948-1998. Solid contours represent intervals of 0.5  $^{\circ}\text{C}$  and dashed lines represent intervals of 0.25.
- Figure 18. Interannual standard deviation ( $^{\circ}\text{C}$ ) of temperature at 900 m depth based on year-season anomaly fields for 1948-1998. Solid contours represent intervals of 0.5  $^{\circ}\text{C}$  and dashed lines represent intervals of 0.25.
- Figure 19. Interannual standard deviation ( $^{\circ}\text{C}$ ) of temperature at 1000 m depth based on year-season anomaly fields for 1948-1998. Solid contours represent intervals of 0.5  $^{\circ}\text{C}$  and dashed lines represent intervals of 0.25.

## Acknowledgments

This work was made possible by a grant from the NOAA Climate and Global Change Program which enabled the establishment of a research group at the National Oceanographic Data Center. The purpose of this group is to prepare research quality oceanographic databases, as well as to compute objective analyses of, and diagnostic studies based on these databases.

The data made available as part of this atlas include the oceanographic data archives maintained by NODC/WDC-A as well as data acquired as a result of the NODC Oceanographic Data Archaeology and Rescue (NODAR) project and the IODE/IOC Global Oceanographic Data Archaeology and Rescue (GODAR) project. At NODC/WDC-A, “data archaeology and rescue” projects are supported with funding from the NOAA Environmental Science Data and Information Management (ESDIM) Program and NOAA Climate and Global Change Program which included support from NASA. The majority of funding for these efforts is now provided by the ESDIM program. Support for some of the regional IOC/GODAR meetings was provided by the MAST program of the European Union (Levitus *et al.*, 1998).

We would like to acknowledge the scientists, technicians, and programmers who have submitted data to national and regional data centers as well as the managers and staff at the various data centers. Our database now allows for the storage of additional metadata including information about Principal Investigators to recognize their efforts as well as to provide information that may be useful in determining the quality of data.

Recent declassification of substantial amounts of naval oceanographic data by the Russian Naval Ocean Research Center, the United Kingdom Hydrographic Office, and the Argentine Navy is acknowledged. The U.S. Navy has been declassifying data on a continuing basis over many years.

We appreciate the efforts of Clara Deser in reviewing the manuscript version of this publication.

# **YEARLY AND YEAR-SEASON UPPER OCEAN TEMPERATURE ANOMALY FIELDS, 1948-1998**

*Sydney Levitus, Cathy Stephens, John Antonov, and Timothy P. Boyer*

Ocean Climate Laboratory  
National Oceanographic Data Center

Silver Spring, MD 20910

## **ABSTRACT**

This atlas describes the computation of upper ocean thermal anomaly fields for 1948-1998 from the surface to 1000 meters depth. It also presents the interannual standard deviation of seasonal temperature anomaly fields for the world ocean for this period. For the region from the surface through 200 meters, the equatorial regions of the world oceans exhibit the standard deviation. The deeper oceans from 500 to 1000 meters exhibit large standard deviation in the Gulf Stream region and in the Agulhas Current region off the southern tip of Africa.

## **1. INTRODUCTION**

We have used historical ocean temperature profile data to prepare yearly and year-seasonal temperature anomaly fields for the 1948-1998 period at standard depth levels in the upper 1000 m of the world ocean. All of the data we have used are available as part of the *World Ocean Database* 1998 (Boyer *et al.*, 1998a,b,c; Levitus *et al.*, 1998a,b) and are available from the National Oceanographic Data Center (NODC) on CD-ROM and on-line.

We have computed the interannual standard deviation of the seasonal temperature anomaly fields at all standard depth levels in the upper 1000 m of the world ocean and present our results in Figs. 1-19.

The following sections include a description of the data, processing techniques, and discussion of the distribution of standard deviation at various depth levels.

## 2. DATA PROCESSING AND OBJECTIVE ANALYSIS

*World Ocean Database 1998, version 1* (1998) temperature data are used to compute seasonal temperature anomaly fields for the periods 1948-1998. Seasonal temperature anomaly fields are calculated similarly to Levitus *et. al.* (1994) (hereafter referred to as L94). Temperature anomaly values at each standard level in each temperature profile were computed by subtracting off the climatological temperature value for the month that the profile was measured in. The climatology used is described by Antonov *et al.* (1998) (hereafter referred to as A98). Data values exceeding three standard deviations from the five-degree square that the data occurred in were not used in creation of the climatology.

Our procedures differ from the work by L94 in one critical way. In our previous preparation of anomaly fields (L94), we did not use any data that exceeded three standard deviations in preparation of our anomaly fields. As part of the present study we computed anomaly fields using all data (as described below) and compared these results with fields based on data that did not include values exceeding three standard deviations. Comparing these fields it became clear that large-scale anomaly features were being reduced in amplitude by the three standard deviation criteria. Therefore, we used a six standard deviation criteria and eliminated other data that created very unrealistic small-scale features (typically bull's-eye patterns with wavelengths less than 500 km).

For each year or year-season compositing all anomaly values were averaged in each one-degree square at each standard depth level from the surface to 1000 m depth. Anomaly fields for each compositing period at each standard depth level were created using a first-guess equal to zero at each grid point. Use of zero as a first-guess rather than persistence or some other procedure minimizes the creation of spurious anomalies. Objective analysis of the one degree-square anomaly means was performed using the same procedures as given by A98. Thus less smoothing was performed in this atlas as compared to the L94 anomaly fields.

When our anomaly fields are averaged their mean is not zero in regions of strong gradients. This is because our interpolation is non-linear. Therefore, the grand mean anomaly from 1948-1998 was subtracted from the data so as not to include computational artifact to the anomaly fields. Although this mean has no effect on the standard deviation fields, it could possibly alter the year-season analysis. The interannual standard deviation of the seasonal anomalies were then computed for the years 1948-1998.



### 3. INTERANNUAL STANDARD DEVIATION

The figures presented in this atlas have a contour interval of  $0.5^{\circ}\text{C}$  (solid lines) with the dashed lines representing intervals of  $0.25^{\circ}\text{C}$  between the main solid lines. At the lower depths, 500 to 1000 meters, the contour  $0.1^{\circ}\text{C}$  is added to the graphs.

The largest magnitudes of standard deviation at 0 to 50 meters depth occur in the equatorial regions of the Pacific Ocean, specifically off the western coast of South America. The magnitudes are as large as  $2.5^{\circ}\text{C}$ . These large magnitudes extend across the entire equatorial region of the world oceans down to 200 meters with the maximum standard deviation of  $2.5^{\circ}\text{C}$  shifting towards the eastern continental boundaries as temperature gradients increase in these regions. These large temperature gradients and increased magnitudes of standard deviation are particularly noticeable in the Indian Ocean from 75 to 150 meters depth and in the equatorial Pacific Ocean from 75 to 200 meters depth (Figs. 6-10, *World Ocean Database 1998*). These large magnitudes in the equatorial regions are associated with the variability of the shallow tropical thermocline.

Another dominant feature with large standard deviations is found off the Cape of Good Hope, the southern tip of Africa. Magnitudes reach  $2.5^{\circ}\text{C}$ , but consistently maintain values of  $2.0^{\circ}\text{C}$  from 0 to 500 meters depth. This region has a complicated current system, most notably associated with the Agulhas current and large temperature gradients are also observed in this region.

However, one region of increased standard deviation values is hypothesized to be the result of lack of data. Large magnitudes of  $2.0^{\circ}\text{C}$  are consistently computed off the southeastern coast of South America from 0 to 500 meters. Although the Brazil and Falklands currents meet in this region, and large temperature gradients are noted, the *World Ocean Atlas 1998* series shows a paucity of data (seasonally) for this region.

Deeper depths exhibit increased standard deviation values off the eastern coast of Japan and in the Gulf Stream region. From 300 to 700 meters, the eastern coast of Japan has maximum standard deviation values ranging from  $1.5$  to  $2.0^{\circ}\text{C}$ , with the largest values computed at 500 meters depth. Although the northern branch of the Gulf Stream, off the coast of Newfoundland, exhibits large variability from 0 to 300 meters, larger standard deviation are found off the entire eastern coast of the United States from 300 to 1000 meters. In the subtropics, the largest area of variability is generally associated with the depth of the main thermocline. At 1000 meters, the two major features of the standard deviation are found off the eastern United States and the southern tip of Africa with magnitudes of  $0.5$  to  $1.0^{\circ}\text{C}$ .

#### 4. SUMMARY

The interannual standard deviation of year-season temperature anomaly fields for the period of 1948-1998 over the world ocean are presented. Temperature anomalies were computed from the analyzed data of the *World Ocean Atlas 1998* series on a  $1^{\circ} \times 1^{\circ}$  grid with a six standard deviation check used to eliminate outliers. In the 0-200 meters depth range, the tropical regions exhibit the largest magnitudes. In the 400-1000 meter depth range, the subtropical regions exhibit largest values. Both cases are the result of the existence of the permanent thermocline and associated vertical temperature gradients in these regions.

#### 5. REFERENCES

- Antonov, J., S. Levitus, T.P. Boyer, M.E. Conkright, T. O'Brien and C. Stephens, 1998: *World Ocean Atlas 1998, Volume 1: Temperature of the Atlantic Ocean*. NOAA Atlas NESDIS 27, U.S. Government Printing Office, Washington, D.C., 166 pp.
- Antonov, J., S. Levitus, T.P. Boyer, M.E. Conkright, T. O'Brien and C. Stephens, 1998: *World Ocean Atlas 1998, Volume 2: Temperature of the Pacific Ocean*. NOAA Atlas NESDIS 28, U.S. Government Printing Office, Washington, D.C., 166 pp.
- Antonov, J., S. Levitus, T.P. Boyer, M.E. Conkright, T. O'Brien and C. Stephens, 1998: *World Ocean Atlas 1998, Volume 3: Temperature of the Indian Ocean*. NOAA Atlas NESDIS 29, U.S. Government Printing Office, Washington, D.C., 166 pp.
- Boyer, T. P., J. Antonov, J., S. Levitus, M. E. Conkright, T. O'Brien, C. Stephens, D. Johnson, and R. Gelfeld, 1998a: *World Ocean Database 1998, Volume 3: Temporal Distribution of Expendable Bathythermograph Profiles*. NOAA Atlas NESDIS 20, U.S. Government Printing Office, Wash., D.C., 170 pp.
- Boyer, T. P., M. E. Conkright, S. Levitus, C. Stephens, T. O'Brien, D. Johnson, R. Gelfeld, 1998b: *World Ocean Database 1998, Volume 4: Temporal Distribution of Conductivity-Temperature-Depth Profiles*. NOAA Atlas NESDIS 21, U.S. Government Printing Office, Wash., D.C., 163 pp.
- Boyer, T. P., M. E. Conkright, S. Levitus, D. Johnson, J. Antonov, T. O'Brien, C. Stephens, and R. Gelfeld, 1998c: *World Ocean Database 1998, Volume 5: Temporal Distribution of Ocean Station Data (Bottle) Temperature-Salinity Profiles*. NOAA Atlas NESDIS 22, U.S. Government Printing Office, Wash., D.C., 108 pp.
- Levitus, S., T.P. Boyer and J. Antonov, 1994: *World Ocean Atlas 1994, Volume 5: Interannual Variability of the Upper Ocean Thermal Structure*, NOAA Atlas NESDIS 5, U.S.

Government Printing Office, Washington, D.C., 176 pp.

Levitus, S., M. E. Conkright, T. P. Boyer, T. O'Brien, J. Antonov C. Stephens, L. Stathoplos, D. Johnson, R. Gelfeld, 1998: World Ocean Database 1998a, Volume 1: Introduction. *NOAA Atlas NESDIS 18*, U.S. Government Printing Office, Wash., D.C., 346 pp.

Levitus, S., T. P. Boyer, M. E. Conkright, D. Johnson, T. O'Brien J. Antonov, C. Stephens, and R. Gelfeld, 1998b: *World Ocean Database 1998, Volume 2: Temporal Distribution of Mechanical Bathythermograph Profiles*. *NOAA Atlas NESDIS 19*, U.S. Government Printing Office, Wash., D.C., 286 pp.

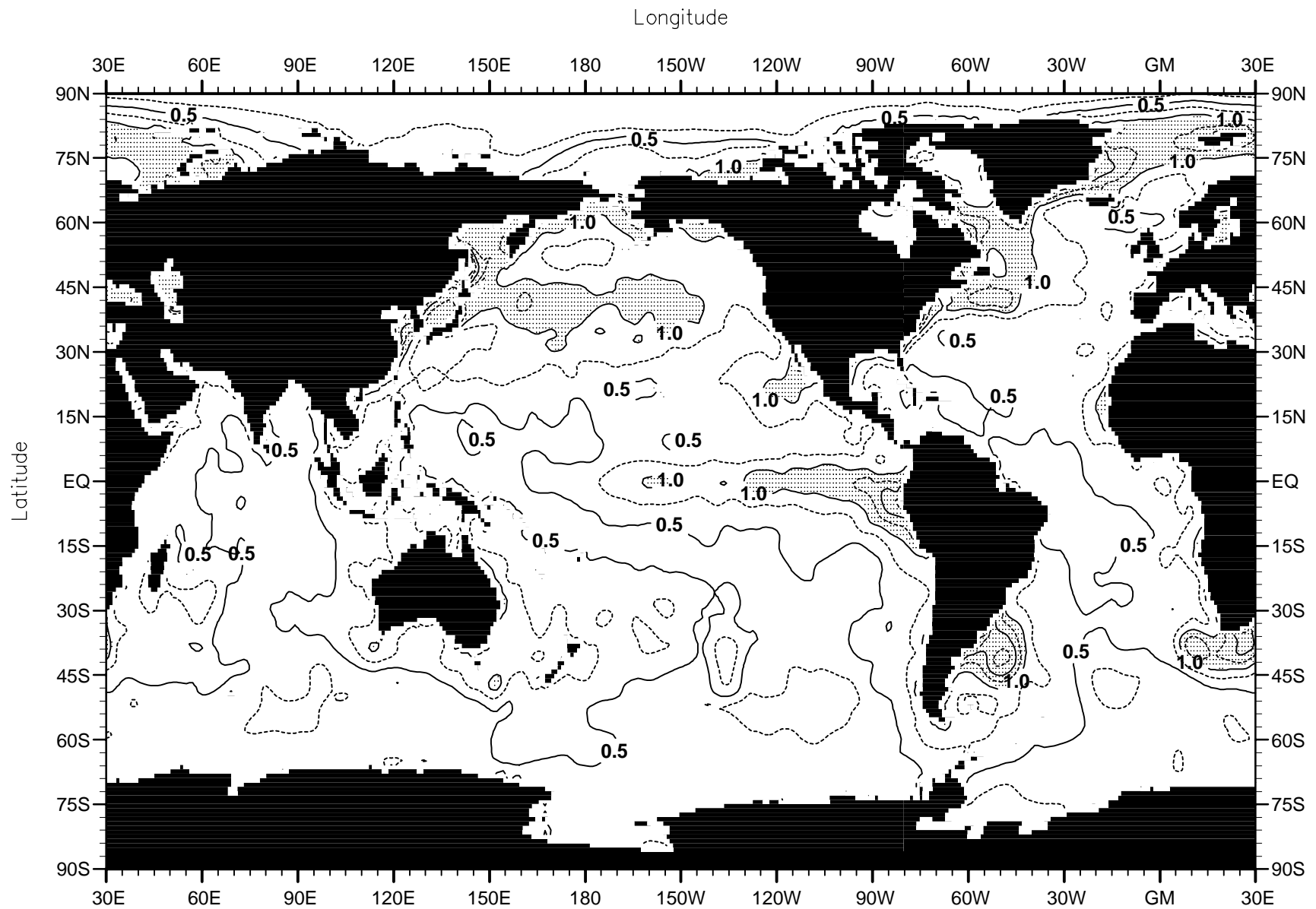


Fig. 1 Interannual std. deviation of seasonal mean temperature ( $^{\circ}\text{C}$ ) anomaly fields for 1948-98 at the sea surface. Solid contours represent intervals of  $0.5^{\circ}\text{C}$  and dashed lines represent intervals of  $0.25$ .

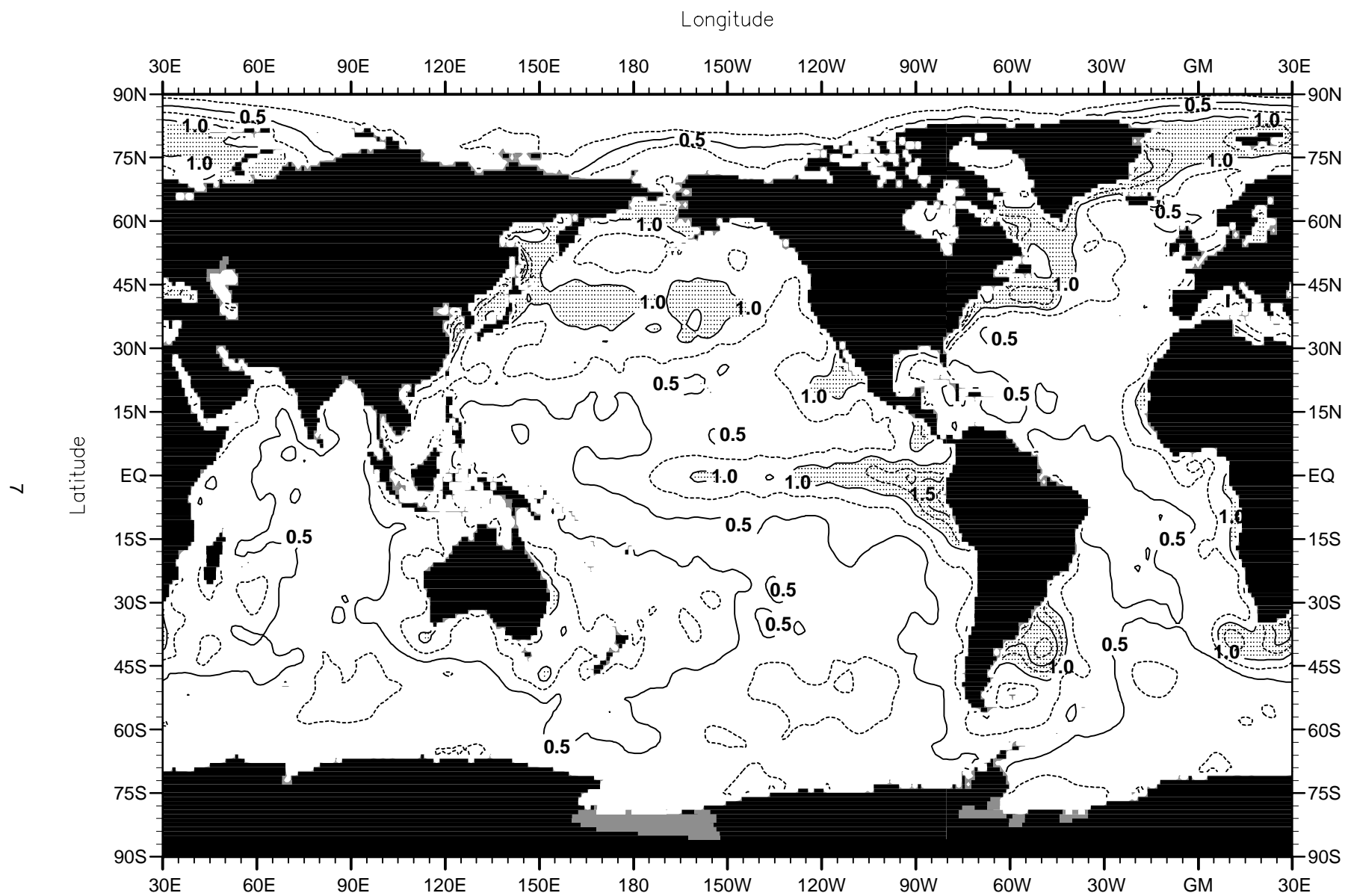


Fig. 2 Interannual std. deviation of seasonal mean temperature ( $^{\circ}\text{C}$ ) anomaly fields for 1948-98 at 10 m depth. Solid contours represent intervals of  $0.5^{\circ}\text{C}$  and dashed lines represent intervals of  $0.25$ .

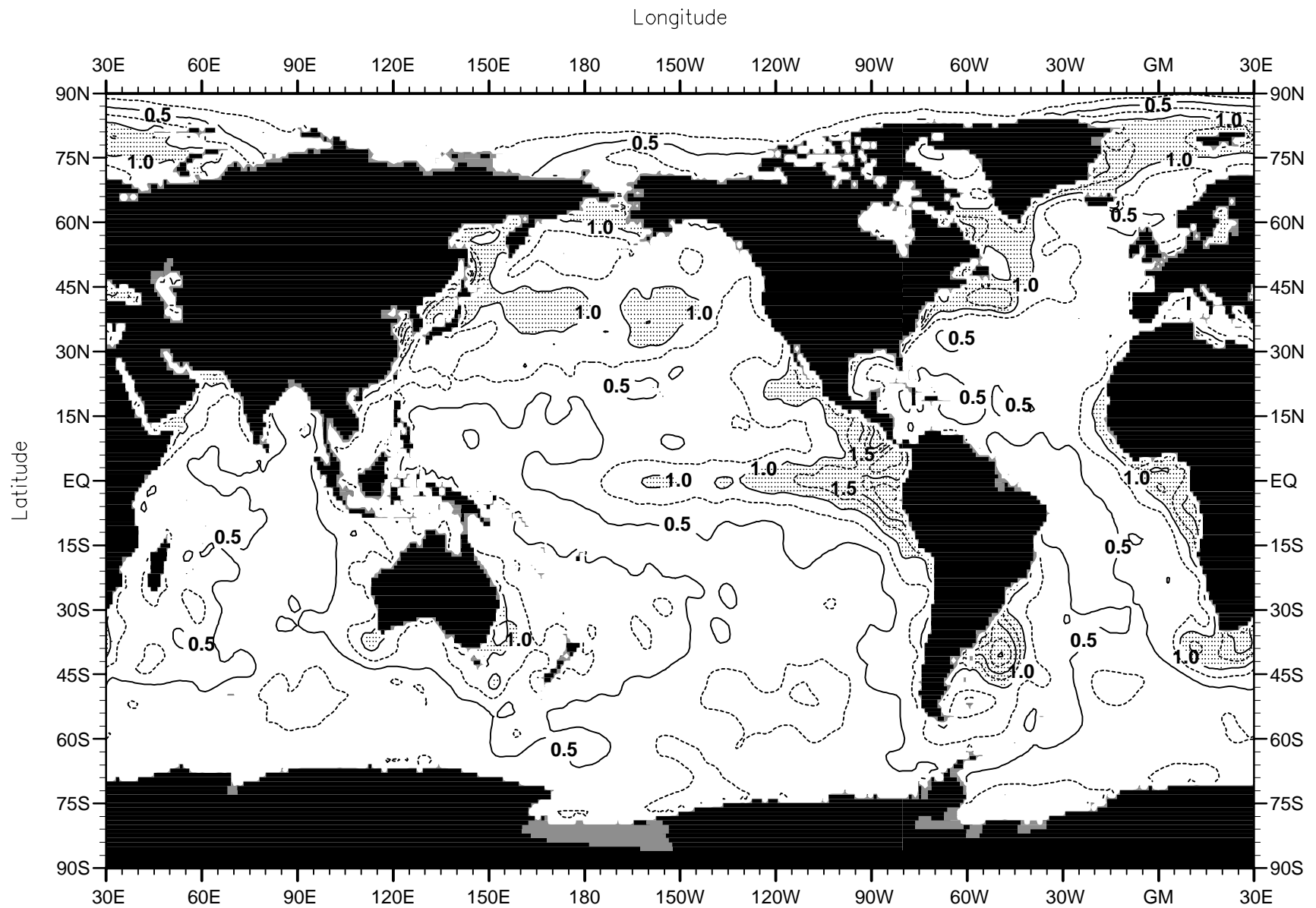


Fig. 3 Interannual std. deviation of seasonal mean temperature ( $^{\circ}\text{C}$ ) anomaly fields for 1948-98 at 20 m depth. Solid contours represent intervals of  $0.5^{\circ}\text{C}$  and dashed lines represent intervals of 0.25.

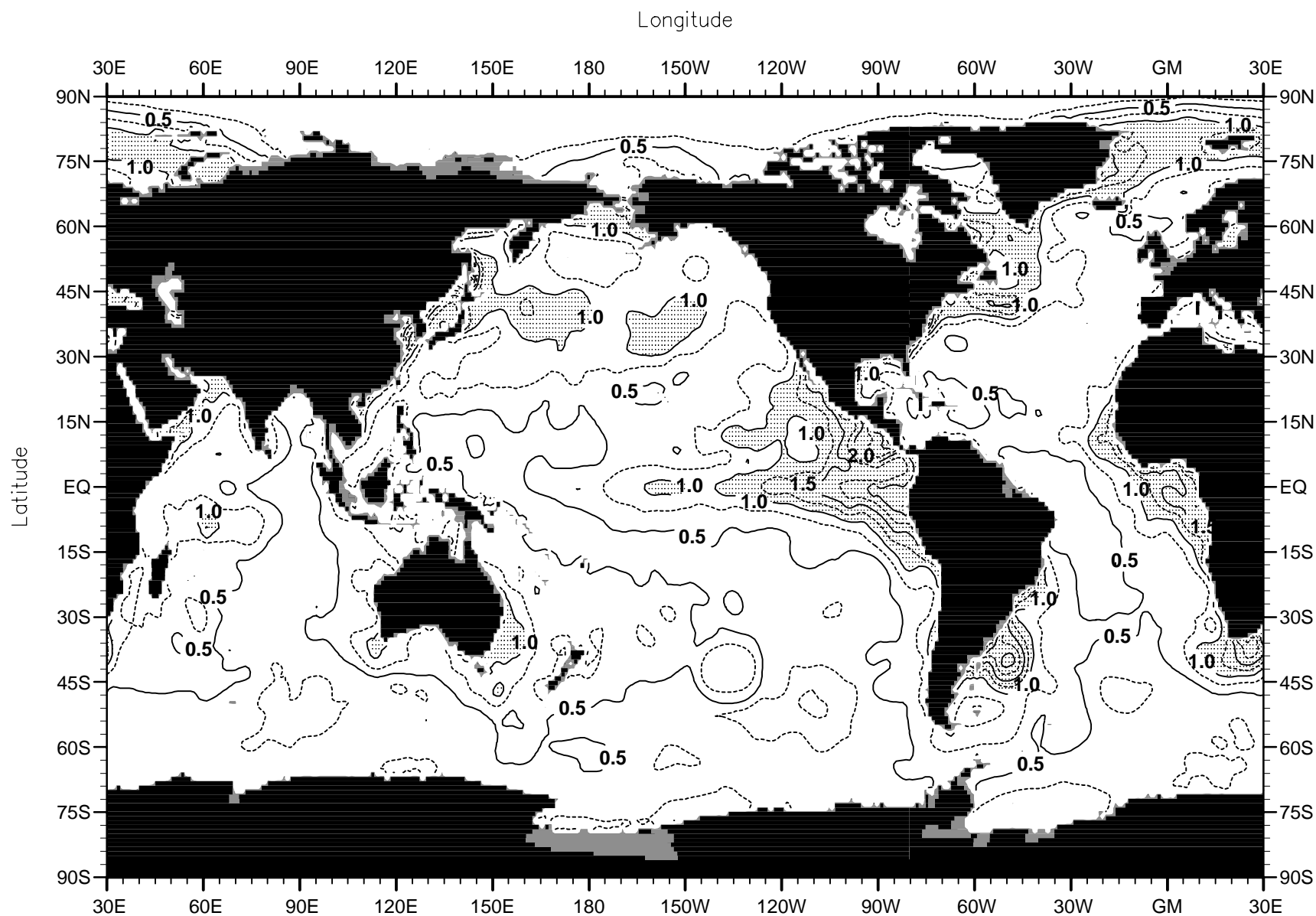


Fig. 4 Interannual std. deviation of seasonal mean temperature ( $^{\circ}\text{C}$ ) anomaly fields for 1948-98 at 30 m depth. Solid contours represent intervals of  $0.5^{\circ}\text{C}$  and dashed lines represent intervals of  $0.25$ .

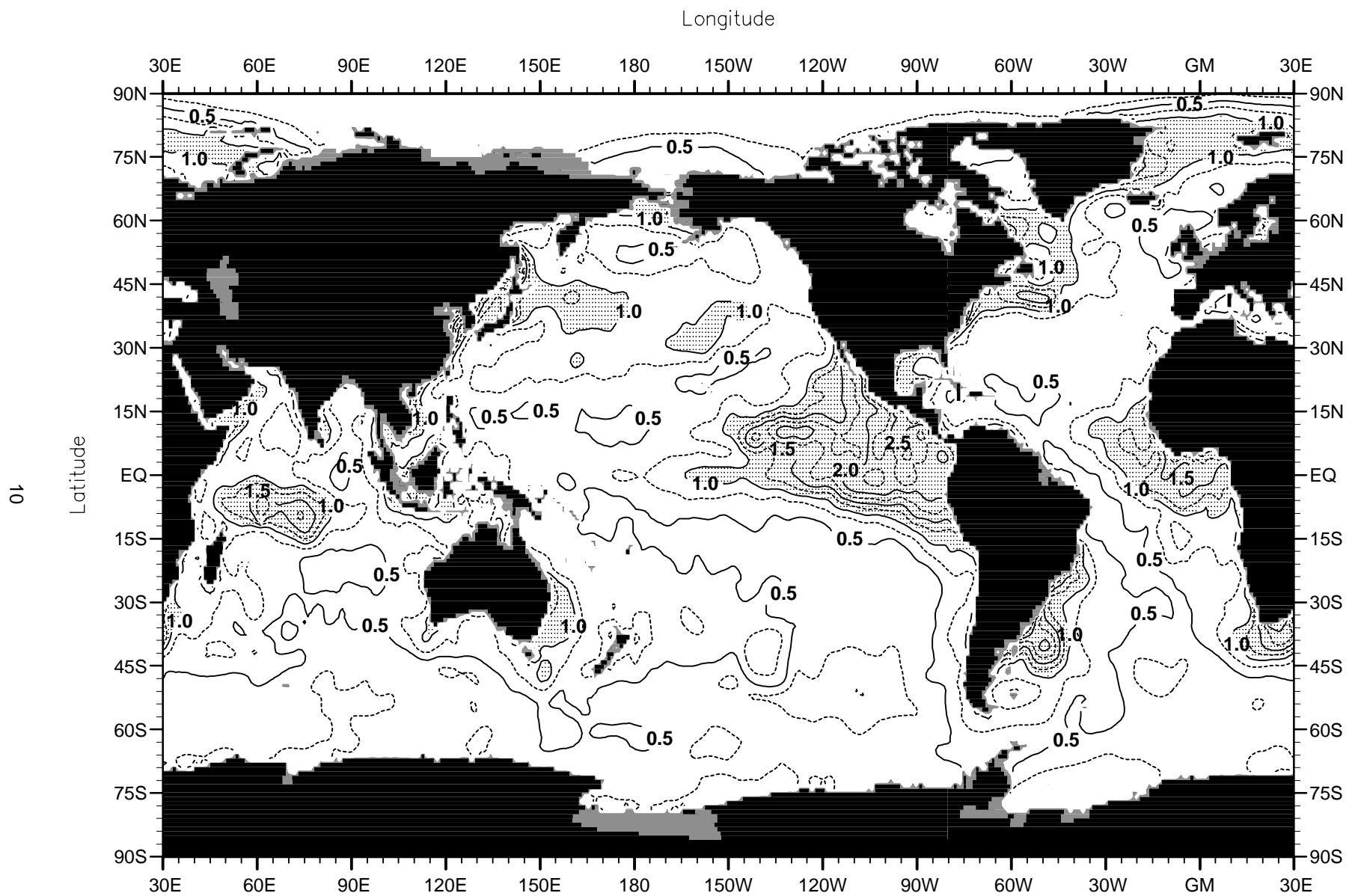


Fig. 5 Interannual std. deviation of seasonal mean temperature ( $^{\circ}\text{C}$ ) anomaly fields for 1948-98 at 50 m depth.  
Solid contours represent intervals of  $0.5^{\circ}\text{C}$  and dashed lines represent intervals of  $0.25$ .



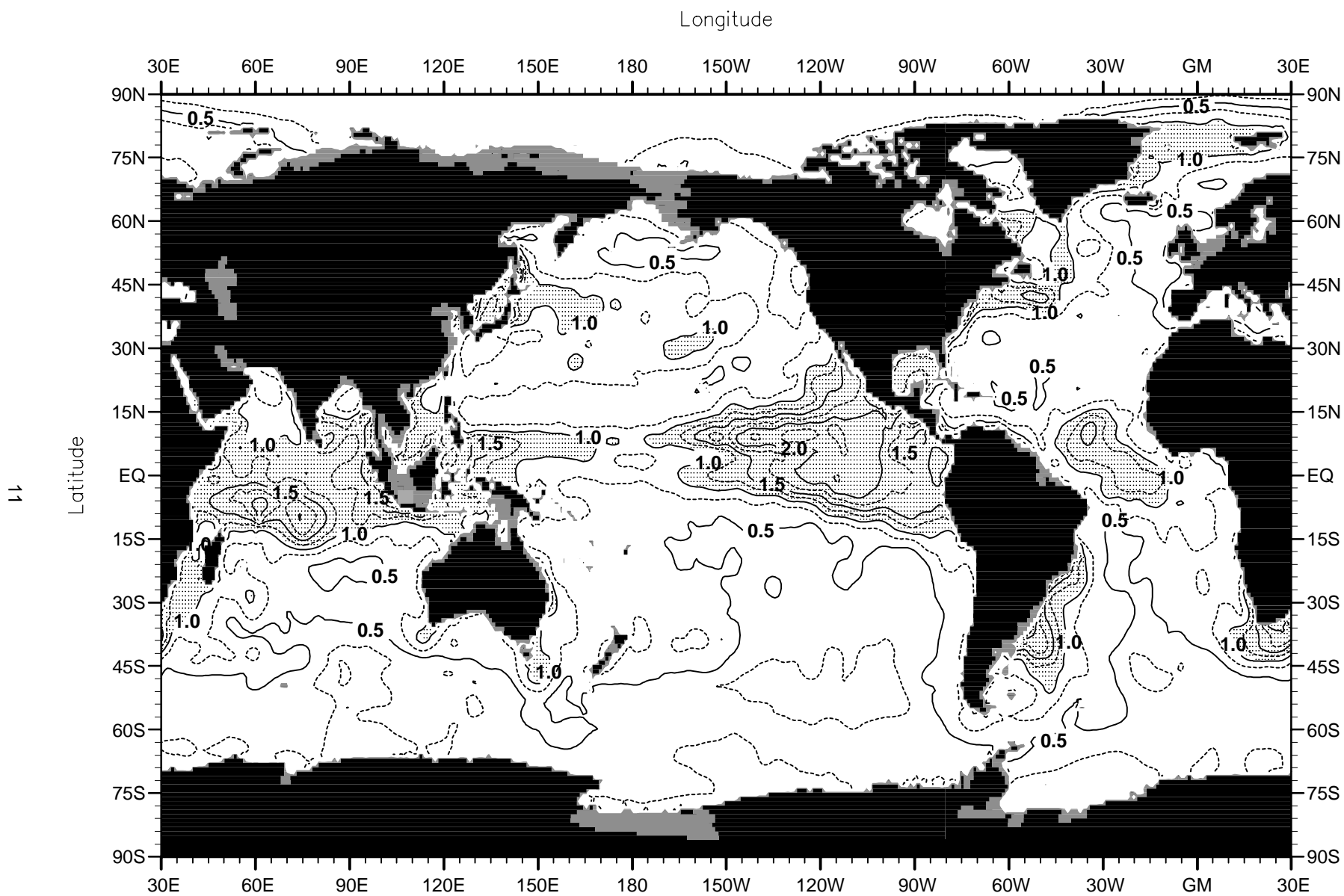


Fig. 6 Interannual std. deviation of seasonal mean temperature ( $^{\circ}\text{C}$ ) anomaly fields for 1948-98 at 75 m depth.  
Solid contours represent intervals of  $0.5^{\circ}\text{C}$  and dashed lines represent intervals of  $0.25$ .

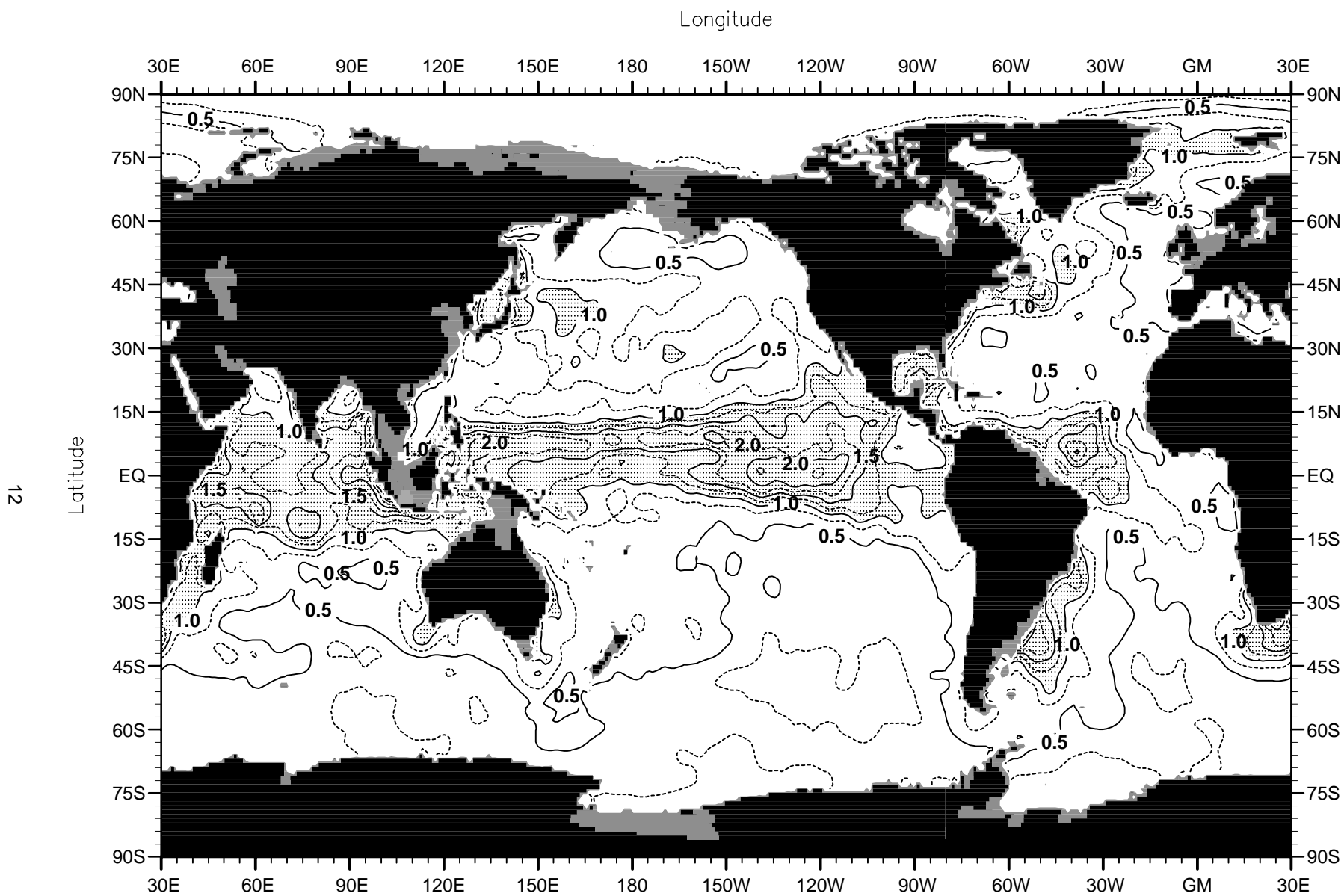


Fig. 7 Interannual std. deviation of seasonal mean temperature ( $^{\circ}\text{C}$ ) anomaly fields for 1948-98 at 100 m depth. Solid contours represent intervals of  $0.5^{\circ}\text{C}$  and dashed lines represent intervals of  $0.25$ .

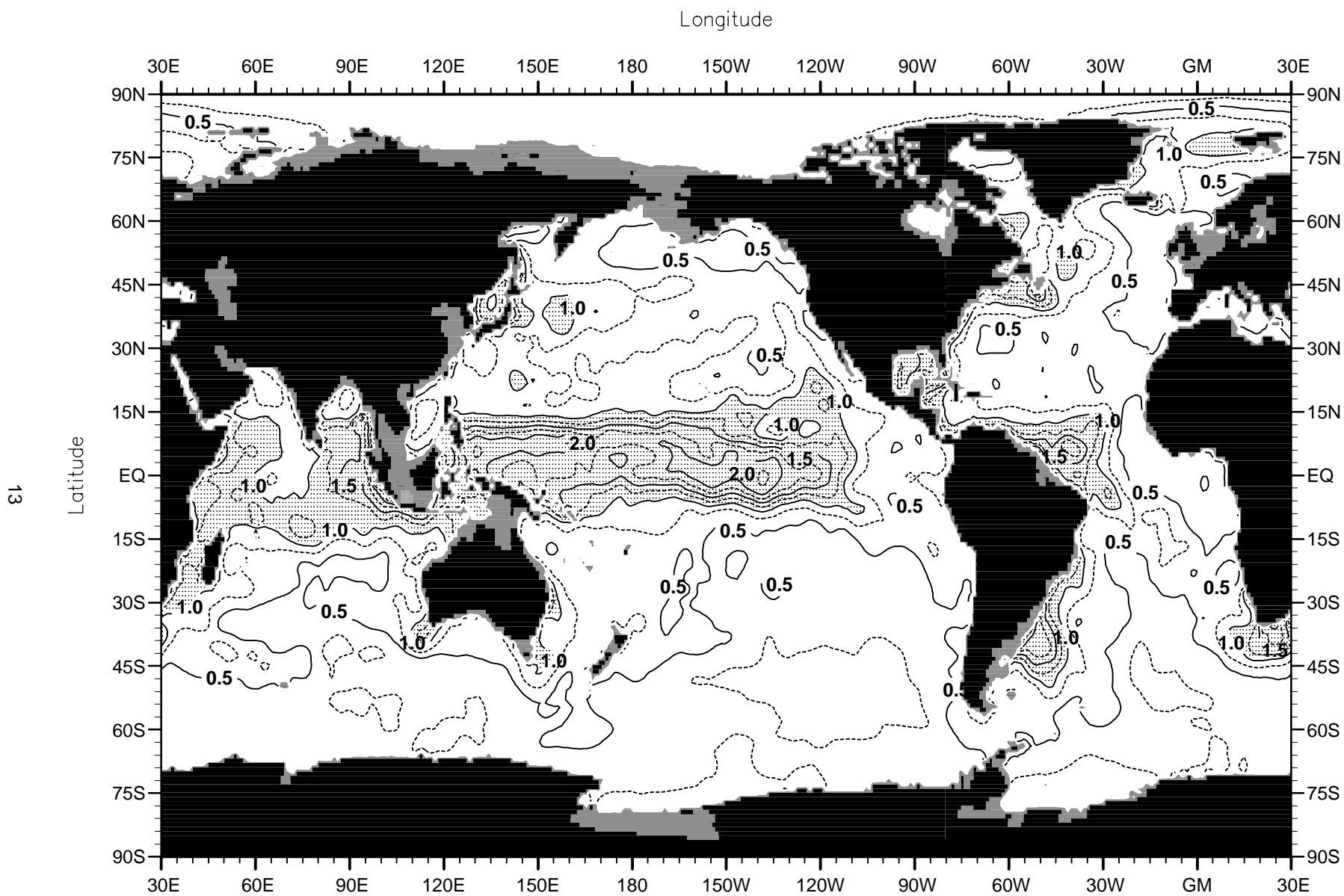


Fig. 8 Interannual std. deviation of seasonal mean temperature ( $^{\circ}\text{C}$ ) anomaly fields for 1948-98 at 125 m depth.  
Solid contours represent intervals of  $0.5^{\circ}\text{C}$  and dashed lines represent intervals of  $0.25$ .

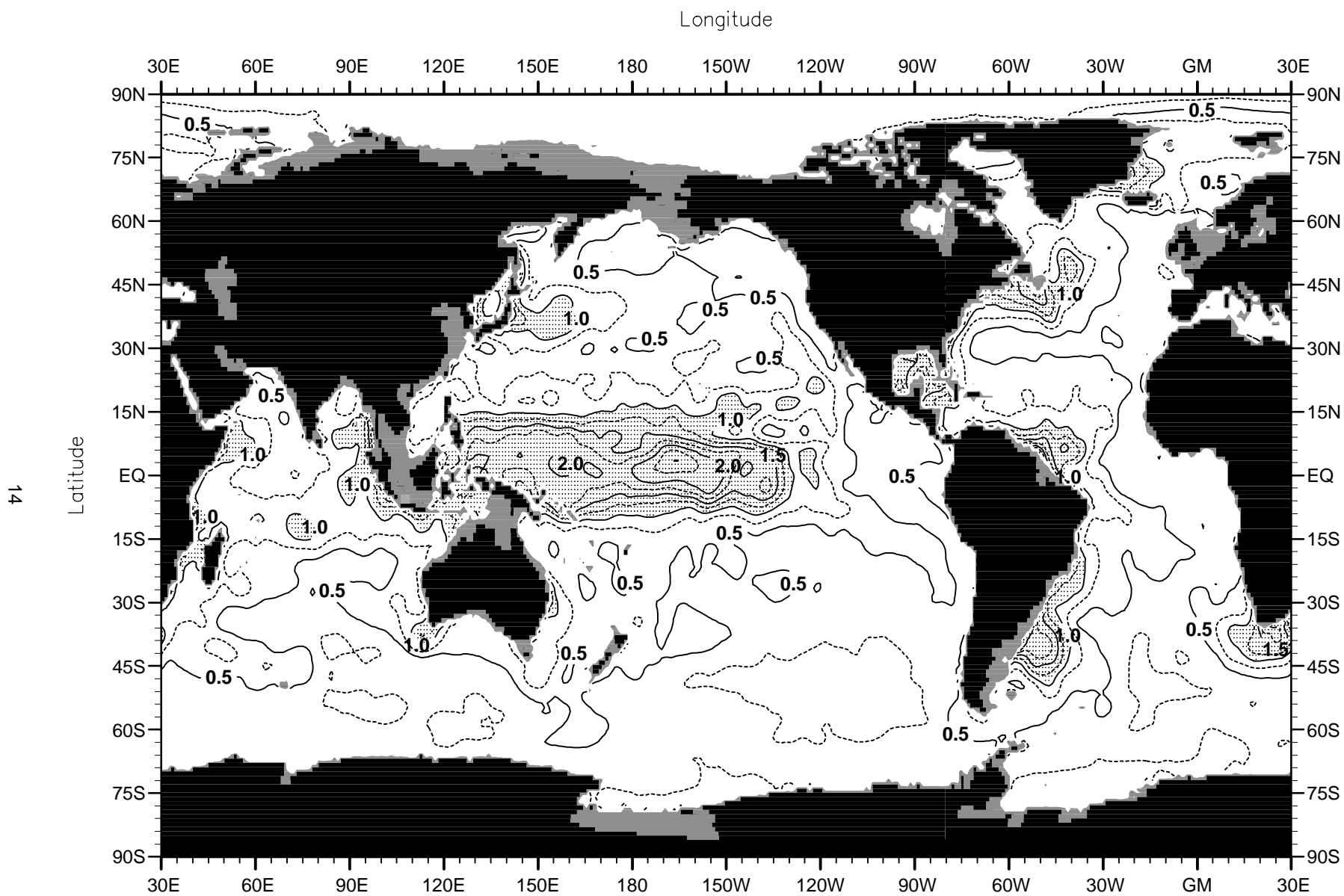


Fig. 9 Interannual std. deviation of seasonal mean temperature ( $^{\circ}\text{C}$ ) anomaly fields for 1948-98 at 150 m depth.  
Solid contours represent intervals of  $0.5^{\circ}\text{C}$  and dashed lines represent intervals of  $0.25$ .

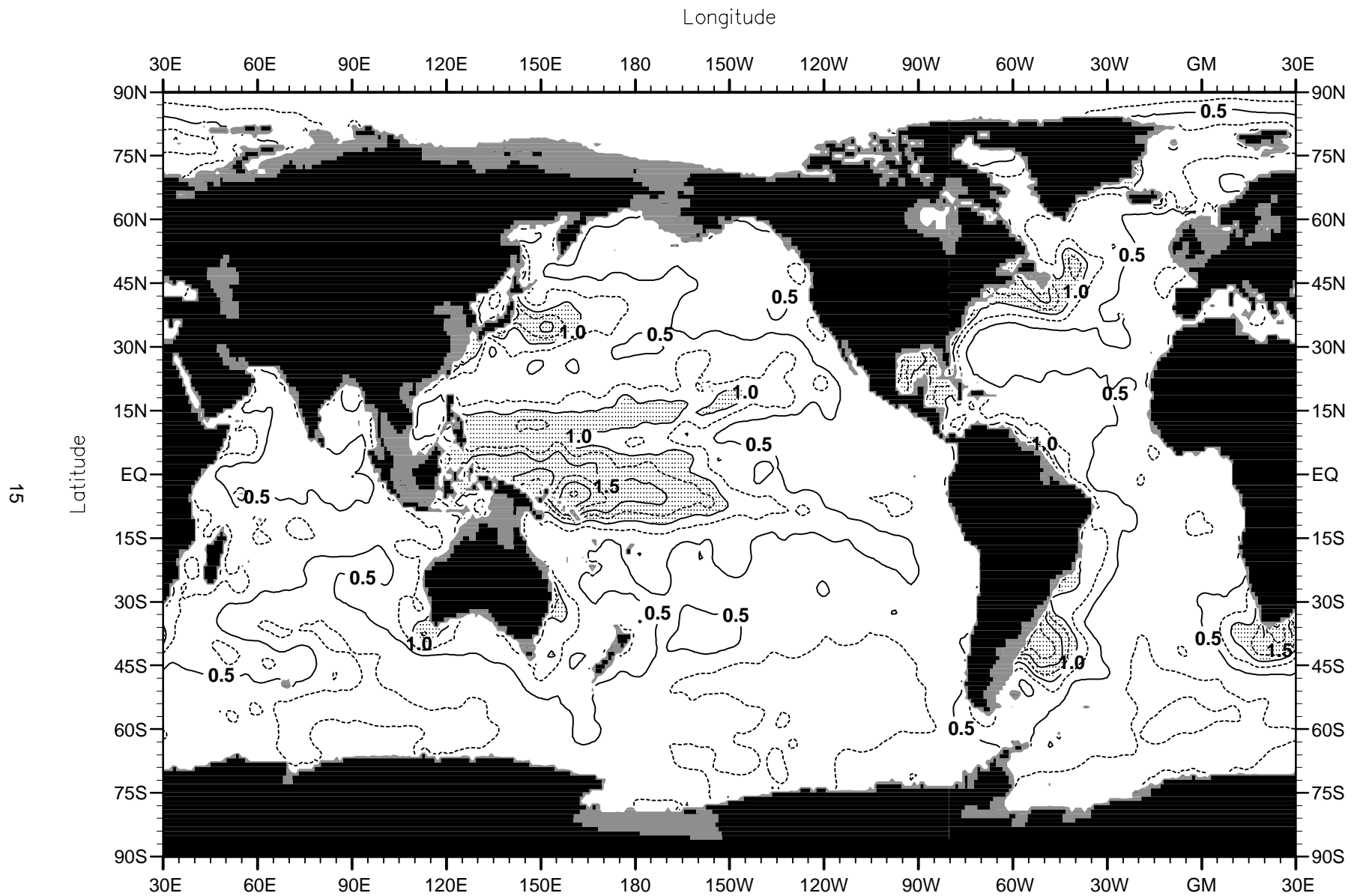


Fig. 10 Interannual std. deviation of seasonal mean temperature ( $^{\circ}\text{C}$ ) anomaly fields for 1948-98 at 200 m depth. Solid contours represent intervals of  $0.5^{\circ}\text{C}$  and dashed lines represent intervals of  $0.25$ .



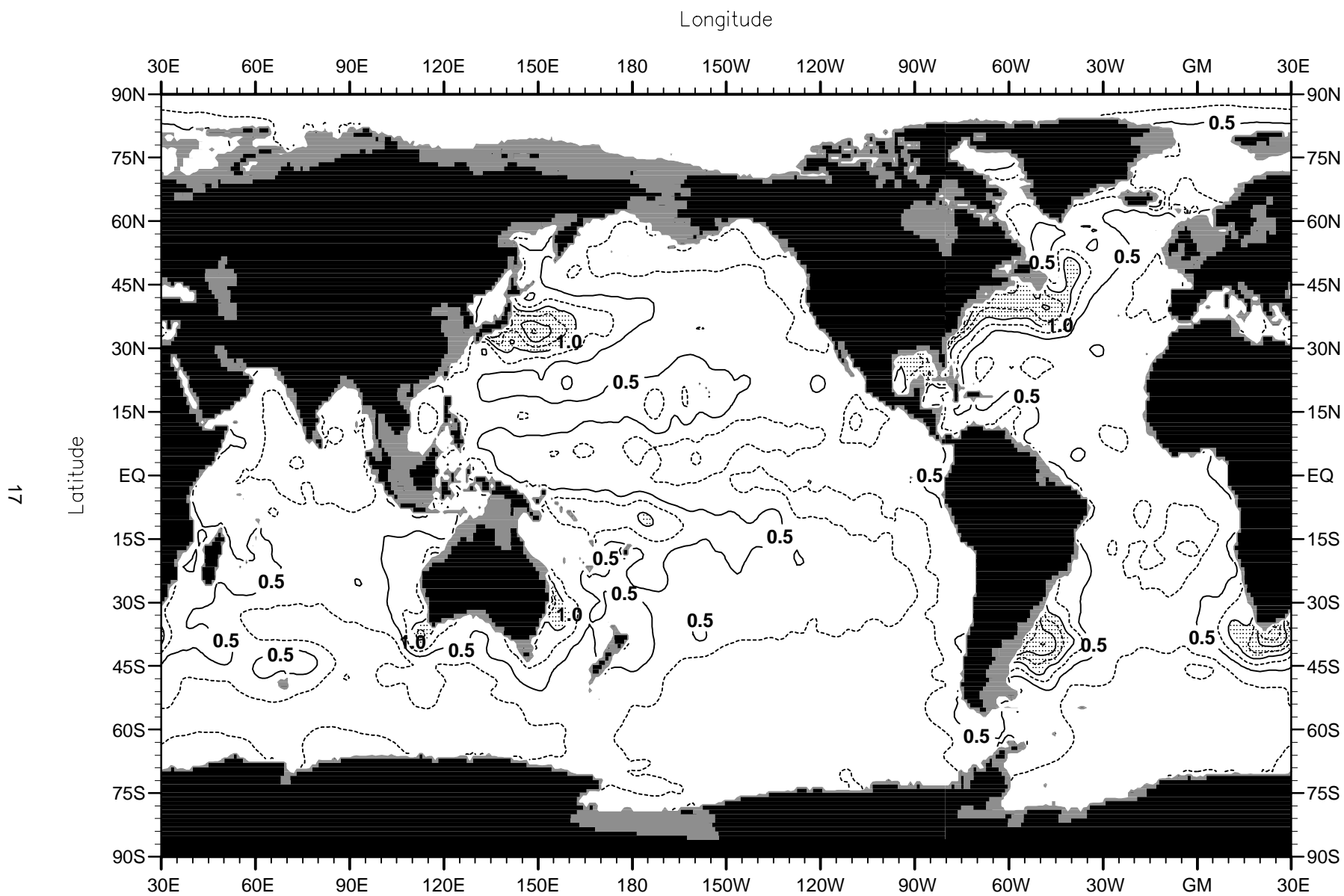


Fig. 12 Interannual std. deviation of seasonal mean temperature ( $^{\circ}\text{C}$ ) anomaly fields for 1948-98 at 300 m depth. Solid contours represent intervals of  $0.5^{\circ}\text{C}$  and dashed lines represent intervals of  $0.25$ .





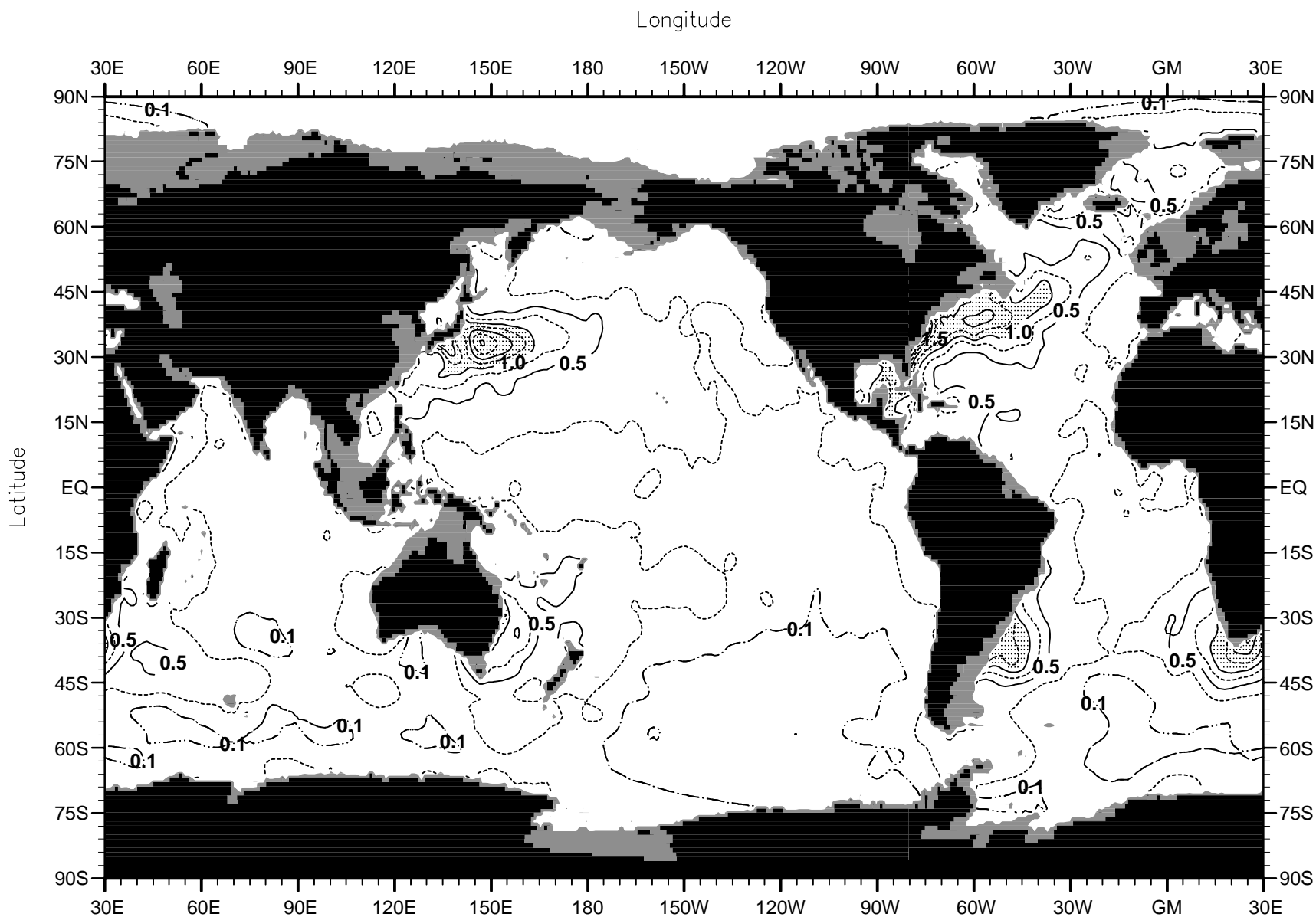


Fig. 14 Interannual std. deviation of seasonal mean temperature ( $^{\circ}\text{C}$ ) anomaly fields for 1948-98 at 500 m depth. Solid contours represent intervals of  $0.5^{\circ}\text{C}$  and dashed lines represent intervals of  $0.25$ .

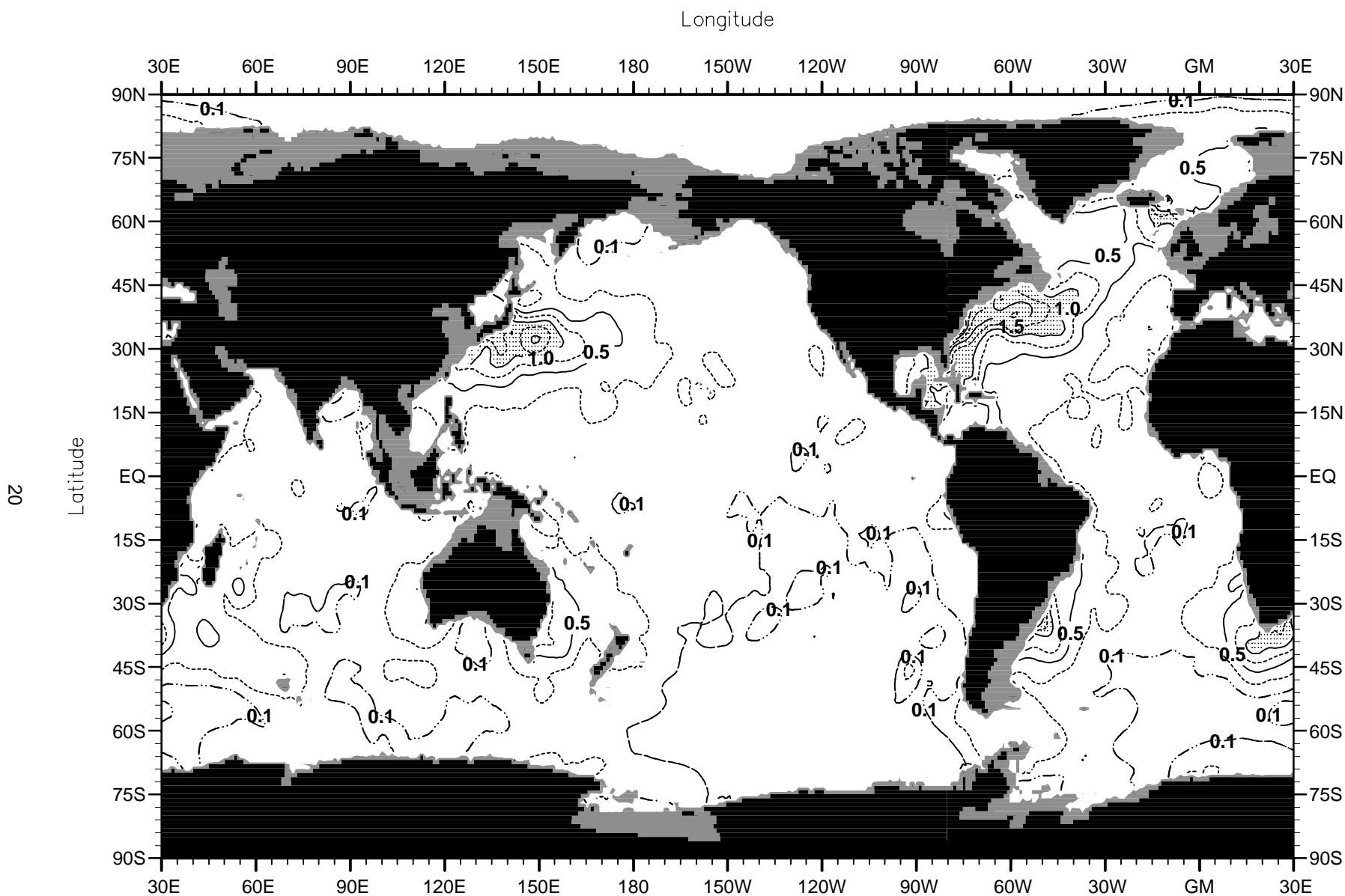


Fig. 15 Interannual std. deviation of seasonal mean temperature ( $^{\circ}\text{C}$ ) anomaly fields for 1948-98 at 600 m depth. Solid contours represent intervals of  $0.5^{\circ}\text{C}$  and dashed lines represent intervals of  $0.25$ .

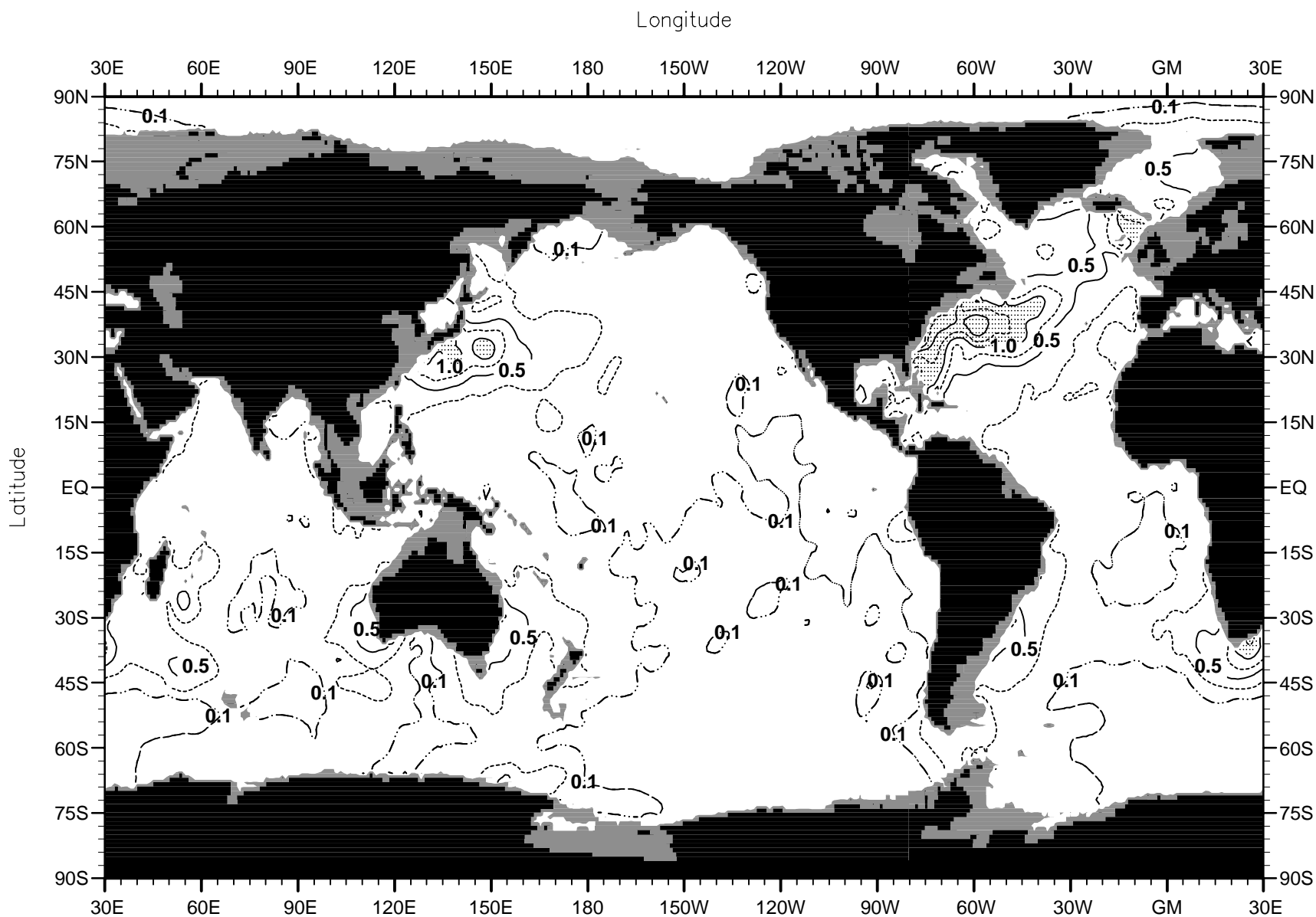


Fig. 16 Interannual std. deviation of seasonal mean temperature ( $^{\circ}\text{C}$ ) anomaly fields for 1948-98 at 700 m depth. Solid contours represent intervals of  $0.5^{\circ}\text{C}$  and dashed lines represent intervals of  $0.25$ .

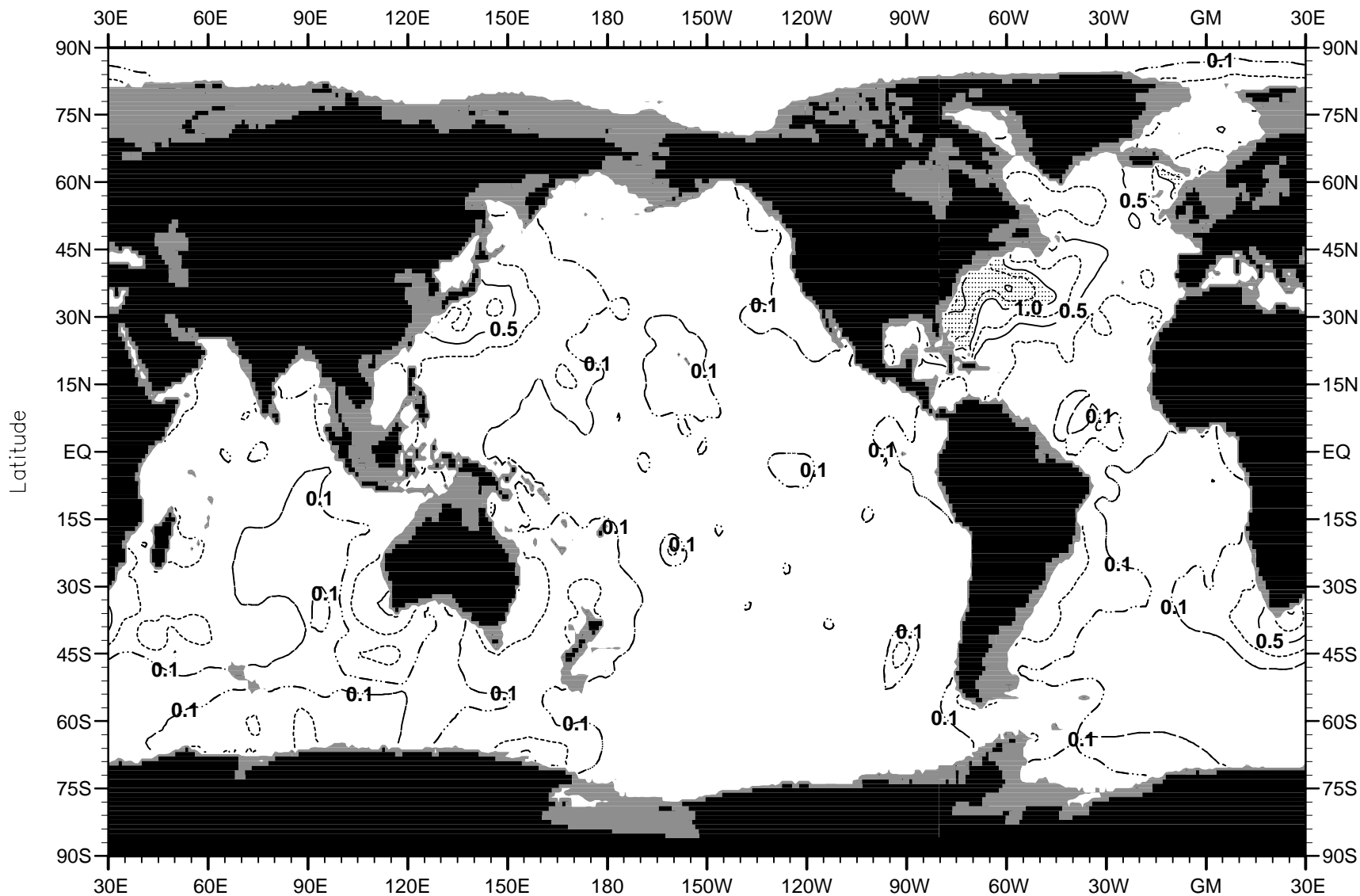


Fig. 17 Interannual std. deviation of seasonal mean temperature ( $^{\circ}\text{C}$ ) anomaly fields for 1948-98 at 800 m depth. Solid contours represent intervals of  $0.5^{\circ}\text{C}$  and dashed lines represent intervals of  $0.25$ .

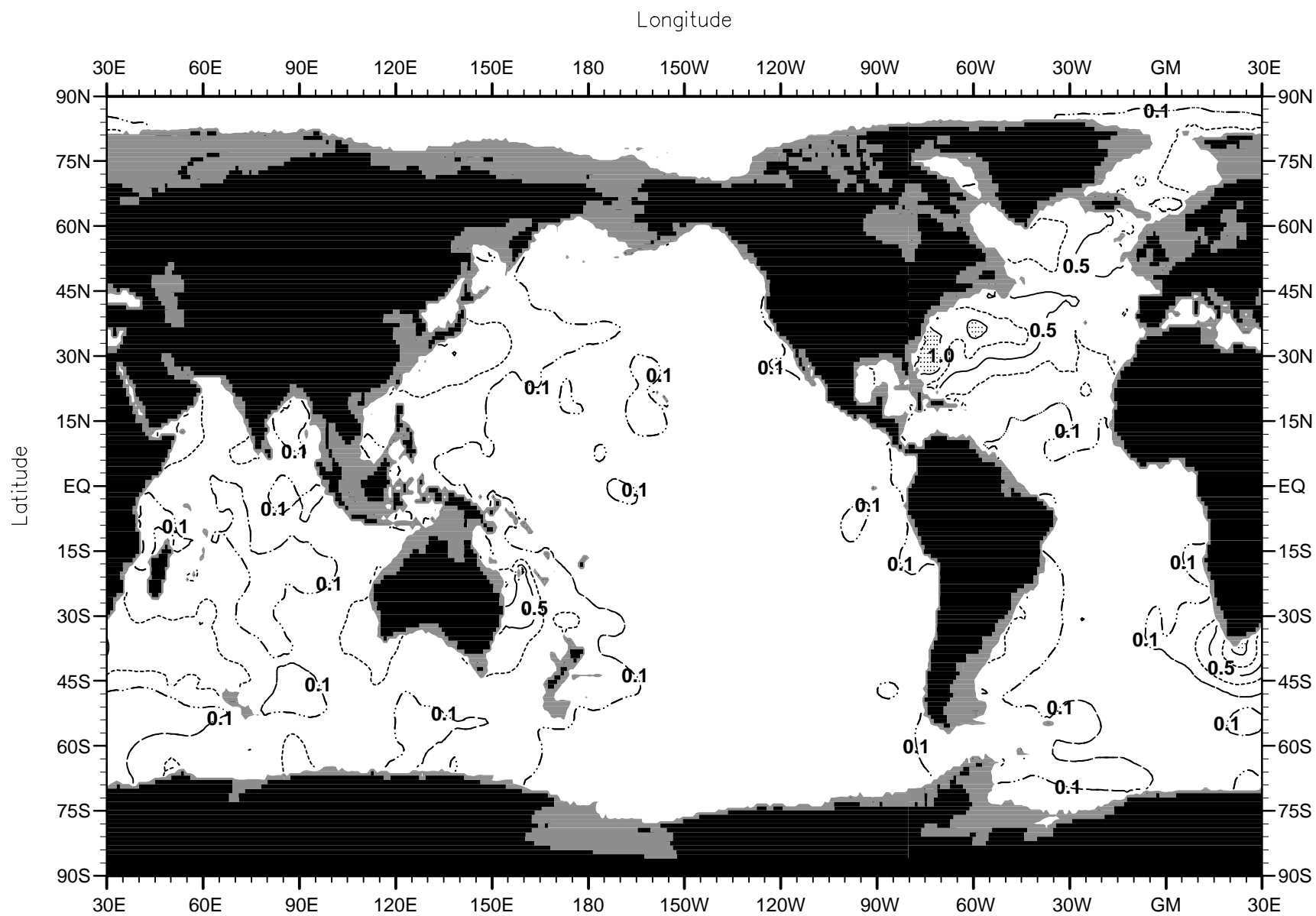


Fig. 18 Interannual std. deviation of seasonal mean temperature ( $^{\circ}\text{C}$ ) anomaly fields for 1948-98 at 900 m depth. Solid contours represent intervals of  $0.5^{\circ}\text{C}$  and dashed lines represent intervals of  $0.25$ .

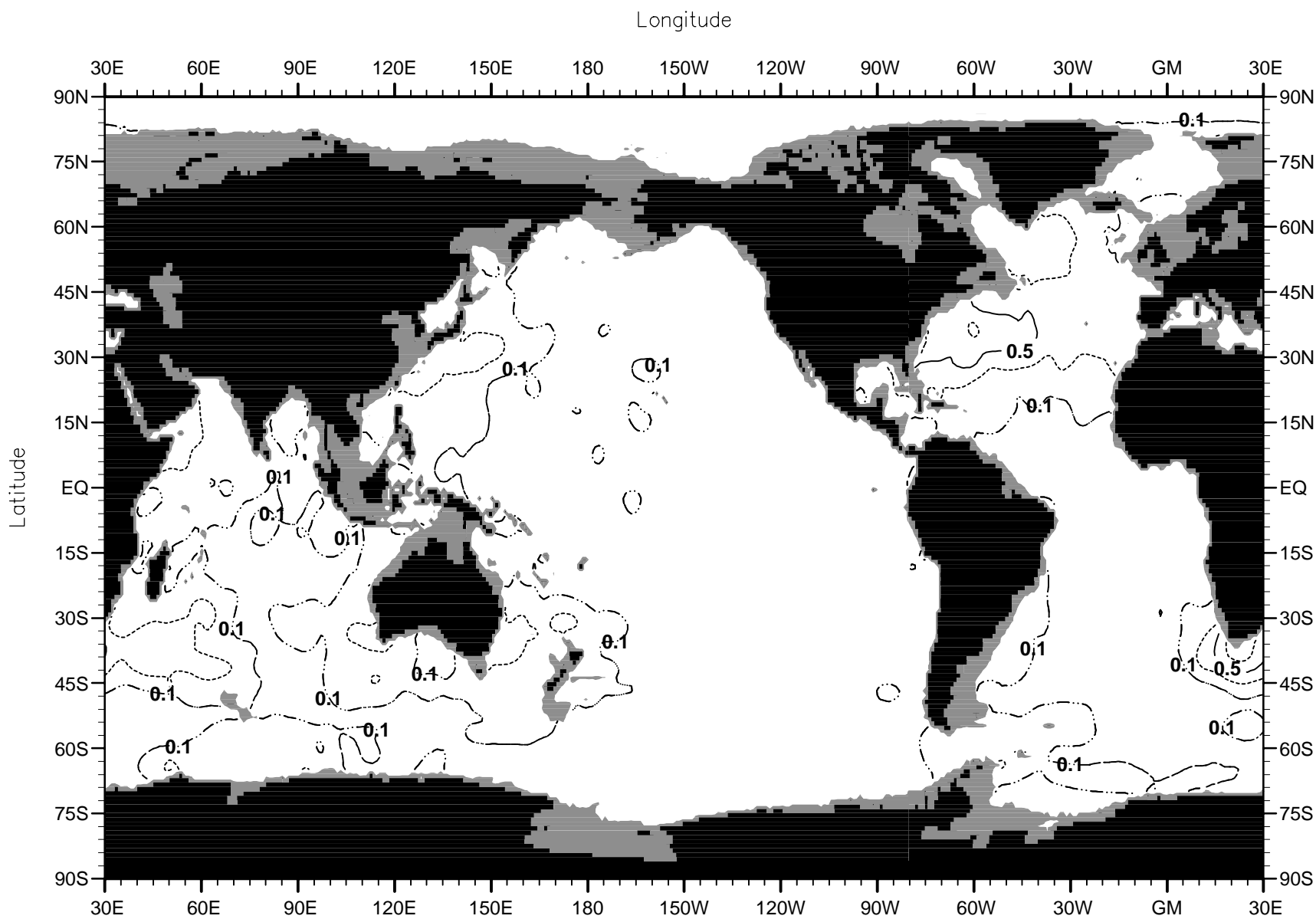


Fig. 19 Interannual std. deviation of seasonal mean temperature ( $^{\circ}\text{C}$ ) anomaly fields for 1948-98 at 1000 m depth. Solid contours represent intervals of  $0.5^{\circ}\text{C}$  and dashed lines represent intervals of  $0.25$ .